ORIGINAL PAPER

Behavior of Cellulose Reinforced Cross-Linked Starch Composite Films Made with Tartaric Acid Modified Starch Microparticles

Iuliana Spiridon · Carmen-Alice Teacă ·
Ruxanda Bodîrlău · Maria Bercea

Abstract Tartaric acid modified starch microparticles (TA-SM) previously obtained using the dry preparation technique were introduced as filler within glycerol plasticized-corn starch (GCS), the composites being prepared by casting process. The effects of cellulose addition within the TA-SM-GCS matrix on the structure, surface properties and water sorption, as well as mechanical and thermal properties of starch-based composite films were investigated. The water resistance and thermal stability were slightly improved through addition of high content of cellulose due to the inter-component H-bonding between components. The evaluation of mechanical properties evidenced a significant increase of the tensile strength of the composites with increasing the content level of cellulose.

Keywords Biopolymers · Starch · Cellulose · Composites · Properties

Introduction

There is a growing interest in developing bio-based products and innovative processing technologies which offer sustainability and mitigation of the dependence on fossil fuel. Among biopolymers, starch is one of the most promising renewable bioresources due to its versatility, competitiveness in price, and applicability to development of new biomaterials with various uses [1–3]. Starch is a high Mw carbohydrate polymer composed of two structural classes, linear amylose and branch chained amylopectin, the basic repeating unit being represented by D-glucose molecules connected by glycosidic bonds. It was found that amylose is responsible for the film-forming capacity [4].

Starch is susceptible to versatile physical and chemical modifications [5, 6]. Cross-linking is an efficient method to modify starch. Because of the multi-carboxyl structure of tartaric acid (TA), it may serve as a cross-linking agent. Cross-linking of starch molecules can potentially reinforce the intermolecular binding by introducing covalent bonds and supplement natural intermolecular hydrogen bonds improving the mechanical properties and water resistance of the resulted films [7]. Through disruption of the molecular chain interactions under specific conditions by the introduction of mechanical and heat energy or by addition of a plasticizing agent (e.g., water, amide, and/or polyols), starch can be processed into thermoplastic materials [8]. Currently, biodegradable plastics are primarily used in food packaging films, shopping bags, and flushable sanitary product backing material [9]. Use of starch-based materials is greatly hindered by its intractable nature, brittleness, water-sensitivity, and poor mechanical strength [10–12]. It has been found that using reinforcing materials within a starch matrix is an effective method to obtain high-performance starch-based biocomposites [2, 13, 14].

The use of natural fibers as a reinforcing phase in biocomposites provides positive environmental benefits with respect to ultimate disposability and raw material use. Natural fibers present very attractive properties such as low cost, renewability, biodegradability, high specific strength and modulus, low density, easy processability and relatively reactive surface for grafting specific groups [14, 15]. Cellulose is the most abundant biopolymer on earth and is present in a wide variety of living species, such as animals, plants, and bacteria. This linear polymer is composed of

I. Spiridon · C.-A. Teacă (✉) · R. Bodîrlău · M. Bercea
Romanian Academy, "Petru Poni" Institute of Macromolecular
Chemistry, 41 A Gr. Ghica Voda Alley, 700487 Iasi, Romania
e-mail: cateaca14@yahoo.com

β-1, 4 linked glucopyranose units, with polymer chains associated by hydrogen bonds forming bundles of fibrils, also called microfibrillar aggregates, where highly ordered regions (i.e., crystalline phases) alternate with disordered domains (i.e., amorphous phases) [16]. Integrated bio-refinery concept provides a promising opportunity and a processing facility that extracts carbohydrates, oils, lignin, and other materials from biomass and converts them into multiple products including fuels and high-value chemicals and materials. Pulp and paper mills are examples of bio-refinery facilities that already produce some combination of industrial and consumer products.

Various types of cellulose fillers such as jute fibers, eucalyptus pulp fibers, flax fiber, tunicin, and ramie fibers, have been prepared and used as reinforcing agents in bio-composites [17, 18]. For use as a packaging material, it is important to study their dynamic mechanical behavior and thermal stability along with their mechanical properties. Although some biodegradable packaging materials have emerged in the market, their use is restricted due to the high cost with production.

The objective of the present work was to obtain less expensive composite materials based on tartaric acid modified starch microparticles, plasticized starch and cellulose and to evaluate how the addition of cellulose fibers influences films properties. Starch-based composite films reinforced with chemically modified starch have a stable structure under ambient conditions, good resistance to water uptake, and better mechanical properties than those without modified starch [19]. The water resistance of starch-based plastics can be improved by adding a small amount of commercial cellulose fibers up to 15 w/w % [20].

Starch microparticles (SM) were prepared using a commercially corn starch, being further modified by reaction with tartaric acid (TA) in order to obtain modified starch microparticles (TA-SM) by the dry preparation technique [21, 22]. The starch composites were prepared using TA-SM as the filler within a glycerol plasticized-corn starch (GCS) matrix by the casting/solvent evaporation process. Subsequently, a cellulose sample originating from a bleached birch industrial pulp was incorporated as different amounts within the TA-SM-GCS matrix as filler. All the components (starch, cellulose, glycerol) have a hydrophilic nature allowing them to adhere well in films due to hydrogen bonding. By addition of modified starch microparticles within the plasticized starch matrix it can be envisaged the improvement of water sensitivity to fulfill requirements for different applications. Nevertheless, this can be achieved probably due to remaining cross-linking activity within the previously prepared modified starch microparticles. A follow-up work may also consider the alkenylsuccinic anhydride (ASA) product, such as octadecenylsuccinic anhydride as hydrophobizing agent within starch-cellulose based matrix. The succinic anhydride moiety may react with hydroxyl moieties on cellulose, through opening the ring structure. One end of the opened ring can form a C–O–C bond with cellulose, while the other end terminates as COOH.

Changes in the starch and modified starch microparticles structure were studied through X-ray diffraction and FTIR spectroscopy. The effects of cellulose addition were investigated through mechanical tests, wettability, and water sorption tests, as well as thermal properties of starch-cellulose composite materials.

Experimental

Materials

Normal corn starch (S), glycerol, tartaric acid (TA) and ethanol were obtained from Chemical Company Iasi (Romania). Natural cellulose (bleached birch pulp obtained from *Betula verrucosa*) was provided by Södra Company (Sweden). Its chemical composition is: cellulose 74.8 %, xylan 23.6 %, glucomannan 1.1 %, and lignin 0.4 %.

Starch Microparticles (SM) and Tartaric Acid-Modified Starch Microparticles (TA-SM) Preparation

Corn starch (S; 10 g) was added into 200 ml of distilled water. The mixture was heated at 90 °C for 1 h for the complete gelatinization of corn starch with constant stirring, and then 200 ml of ethanol was added dropwise to the solution of gelatinized starch solution with constant and vigorous stirring. When the resulting starch microparticles (SM) suspensions were cooled at the room temperature, another 200 ml of ethanol was added dropwise for about 50 min with constant stirring. The suspensions were centrifuged at 8,000 rpm for 20 min, and the settled SM was washed using ethanol to remove the water. After complete washing, the SM was dried at 50 °C to remove ethanol.

Tartaric acid TA (20 g) was dissolved in 100 ml of ethanol. SM (3.5 g) was mixed with 15 ml of TA solution in a glass tray and conditioned for 12 h at room temperature to allow the absorption of TA solution by SM. The tray was dried in vacuum at about 2 mmHg and 50 °C for 6 h to remove ethanol. The obtained mixture was ground and dried in a forced air oven for 1.5 h at 130 °C. The dry mixture was washed three times with water to remove non-reacted TA. TA-SM mixtures were finally washed with ethanol to remove water, dried at room temperature, and ground. TA-SM can be used as a reinforcing agent for glycerol-plasticized starch because it is not gelatinized during the processing of the composites.

Tartaric Acid Modified Starch Microparticles/ Plasticized Starch/Cellulose Composite Preparation

Tartaric acid modified starch microparticles (TA-SM) were dispersed in a solution of distilled water (100 ml) and glycerol (1.5 g) for 1 h before adding 5 g corn starch and birch cellulose. TA-SM filler loading level (4 wt %), as well as the cellulose loading level (10, 20 and 30 % respectively) was based on the amount of starch. The mixture was heated at 90 °C for 0.5 h with constant stirring in order to plasticise the corn starch. To obtain the TA-SM/ S/cellulose composite films, the mixture was cast using a fast coating technique namely the doctor blade technique. Films were obtained by dropping and spreading the mixture on a glass plate using a blade with a slit width of 0.8 mm. After degassing in a vacuum oven at 50 °C for 24 h up to constant weight, the films were air cooled and detached from the glass surface to be investigated. Films with a thickness of ∼ 0.2 mm were obtained, this value resulting from measurements by means of a digital micrometer. The composite materials, coded as TA-SM/S/ C10, TA-SM/S/C20, respectively TA-SM/S/C30, were preconditioned in a climate chamber at 25 °C and 50 % RH for at least 48 h prior to the mechanical testing. Water content of the composite films was around 9 wt %.

X-ray Diffraction

The crystalline structure of the S, SM and TA-SM was studied by XRD using a Bruker AD8 ADVANCE X-ray diffractometer with Cu Kα radiation at 60 kV and 50 mA, at room temperature. Scattered radiation was detected in the diffraction angle 2θ ranging from 10 to 30° at a rate of $2°\ min^{-1}$.

Fourier Transform Infrared (FTIR) Spectroscopy

FTIR spectra of composites were recorded on a Bruker Vertex 70 spectrophotometer. The spectral resolution was $4\ cm^{-1}$ and the scanning range varied from 400 to $4,000\ cm^{-1}$.

Film Opacity

The composites opacity was measured by a JENWAY 6405 UV–Vis spectrophotometer and defined as the area under the absorbance spectrum between 400 and 800 nm according to the ASTM D 1003-00 method (ASTM D 1003-00 Standard Test Method for Haze and Luminous Transmittance of Transparent Plastics). The film samples were cut into a rectangular piece (1 × 2.5 cm, 0.2 mm thickness), fixed on the inner side of a 1 cm spectrophotometer cell and the absorbance spectrum recorded. The film opacity determinations were repeated three times.

Contact Angle Measurements

The films were kept 48 h at 50 % RH before being tested in static conditions on a KSV CAM 200 goniometer. A 2.5 µl droplet of water was applied on the film surface. The evolution of the droplet shape was recorded every second by a video camera and image analysis software was used to determine the contact angle. Water and ethylene glycol were employed as liquids with different polarity. The value reported is the average of ten measurements.

Water Uptake Measurements

To determine the water absorption [20], the composite materials specimens used were thin rectangular strips with dimensions of 10 mm × 10 mm × 0.2 mm. The films were supposed to be thin enough so that the molecular diffusion was considered to be one-dimensional and were vacuum-dried at 90 °C overnight. After weighing, they were conditioned at 25 °C in a desiccator containing sodium sulfate in order to ensure a relative humidity (RH) of 95 %. They were then removed at specific intervals and gently blotted with tissue paper to remove the excess of water on the surface, and the water uptake was calculated with Eq. 1, as follows:

$$\text{water uptake } (\%) = [(W_t - W_0)/W_0] \times 100 \qquad (1)$$

where: W_t and W_0 represents the weight at time t and before exposure to 95 % RH, respectively. The determinations were performed in triplicate.

Mechanical Properties

Tensile stress and strain at break were evaluated according to ASTM D882-00 (ASTM D882-00 Standard Test Method for Tensile Properties of Thin Plastic Sheeting) using an Instron 3345 with a 5-kN load cell. Before testing, the films were cut into strips and conditioned at 50 % RH and 25 °C for 48 h. Testing was done on samples each measuring 10 cm × 1 cm randomly cut from the cast films. The thickness of each specimen was measured at four points along its length with digital micrometer. The crosshead speed was 10 mm/min. A minimum of 10 replications of each test sample were run.

Thermal Properties

DSC measurements were performed under nitrogen atmosphere by means of Mettler- Toledo differential scanning calorimeter DSC1 (Mettler-Toledo, USA). Samples were heated from 0 to 250 °C at a rate of 10 °C/min (first heating), cooled to 0 °C from 250 °C at the same rate (cooling), and then heated again to 250 °C at 10 °C/min (second heating). The instrument was calibrated with

indium (melting point 156.4 °C) and an empty pan was used for reference. Samples (10 mg each) were hermetically sealed in aluminum sample pans. The DSC cell was flushed with nitrogen at a flow rate of 20 ml/min to maintain an inert environment. The transition temperatures (onset, peak) were determined from the thermograms obtained for the composite samples according to ASTM D-3418 (ASTM D-3418 Standard Test Method for Transition Temperatures and Enthalpies of Fusion and Crystallization of Polymers by Differential Scanning Calorimetry). Sample means were calculated from three individually prepared films as the replicated experimental units.

TG/DTG analysis was performed using a Netzsch STA 449 F1 Jupiter system under nitrogen atmosphere. The measurements were performed while heating the samples (≈ 5 mg) placed in Al_2O_3 crucibles hermetically closed with lids at a rate of 10 °C/min from room temperature up to 600 °C and using nitrogen as a purging gas at a flow rate of 50 ml/min. TG curves recorded with a ± 0.5 °C precision were analyzed using a Netzsch Proteus analysis software.

Results and Discussion

X-ray Diffraction

Corn starch is a semi-crystalline material which presents sharp diffraction peaks of A-type starch at of 15.3°, 17.5°, and 23.1° (2θ). In the gelatinization processing, glycerol and water molecules entered into starch granules, and replaced starch intermolecular and intramolecular hydrogen bonds and destructed the crystallinity of starch. There was no obvious starch crystallinity in glycerol-plasticized starch. The diffraction peaks for SM and TA-SM look like a V-type starch structure, which is different from A-type diffraction pattern in corn starch, as it is shown in Fig. 1. However, the gelatinized starch shows a V-type starch pattern with diffraction peaks at 13.56°, 20.88° and 22° (2θ). The A-type crystallites are formed by parallel-packed double helices, while V-type crystallites relate to single helical complexes [23]. This variation of crystal pattern suggests that the original starch crystals have been destroyed by gelatinization and new crystals are formed when the paste was precipitated, reflecting the high cohesion and strong hydrogen bonding of the gelatinized starch in the presence of plasticizer (glycerol) and water. An amorphous hill accompanied by very weak crystalline peaks is apparent in the diagram of modified starch, indicating a high ratio of amorphous structure and low crystallization, and proving that the addition of tartaric acid effectively prevented the regular packing of the modified
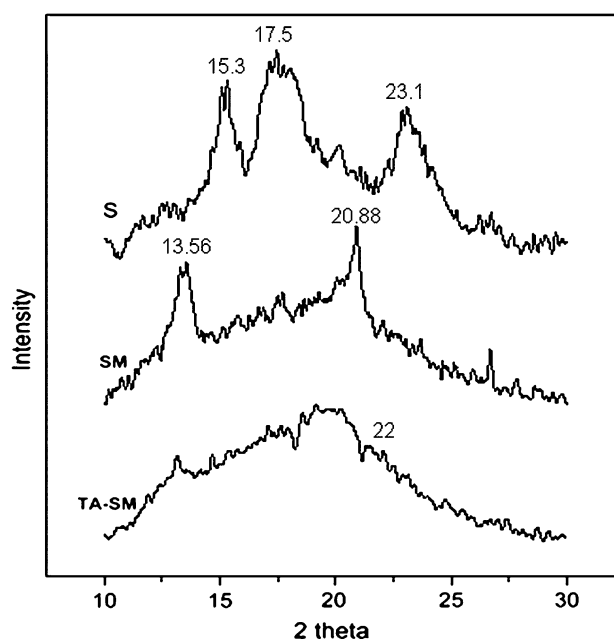

**Fig. 1** XRD diffractograms recorded for S, SM, and TA-SM powders

starch. TA-SM presented a diffraction peak at 22° (2θ) which appeared as diffusion peak of tartaric acid modified starch. The XRD indicated that during starch modification process, several crystalline structures of native starch were destroyed, and a new structure of tartaric acid modified starch was formed (Fig. 1). The diffraction peaks of native corn starch decreased in intensity by addition of TA.

This could be due to the single helical structure ''inclusion complex'' made up of amylose and plasticizer [24]. A similar V-style crystallinity also appeared in the plasticized corn starch. The gelatinization destroyed A-style crystallinity of corn starch by reducing the ability of starch macromolecules to crystallize, and SM exhibited the V-style crystallinity. When TA penetrated the SM granule, it could disrupt to a less extent the V-style crystalline structure of starch, the reaction occurring in the amorphous phase. Substitution of TA groups on starch chains could form a highly cross-linked starch and thus limit starch chain mobility.

FTIR Spectroscopy

The FTIR spectra of components and films are presented in Fig. 2a, b. Figure 2a showed the FTIR spectra of S, SM and TA-SM powders, as well as the spectrum recorded for birch cellulose. Corn starch and SM exhibited similar FTIR spectra. It can be observed that several noticeable changes occur in the spectra of SM and TA-SM. The characteristic peak occurred at 1,650 cm^{-1}, considered to be a feature of tightly bound water present in the starch [25].

Fig. 2 FTIR spectra obtained for components: S, SM, TA-SM, C (**a**) and starch-cellulose composite films (**b**)
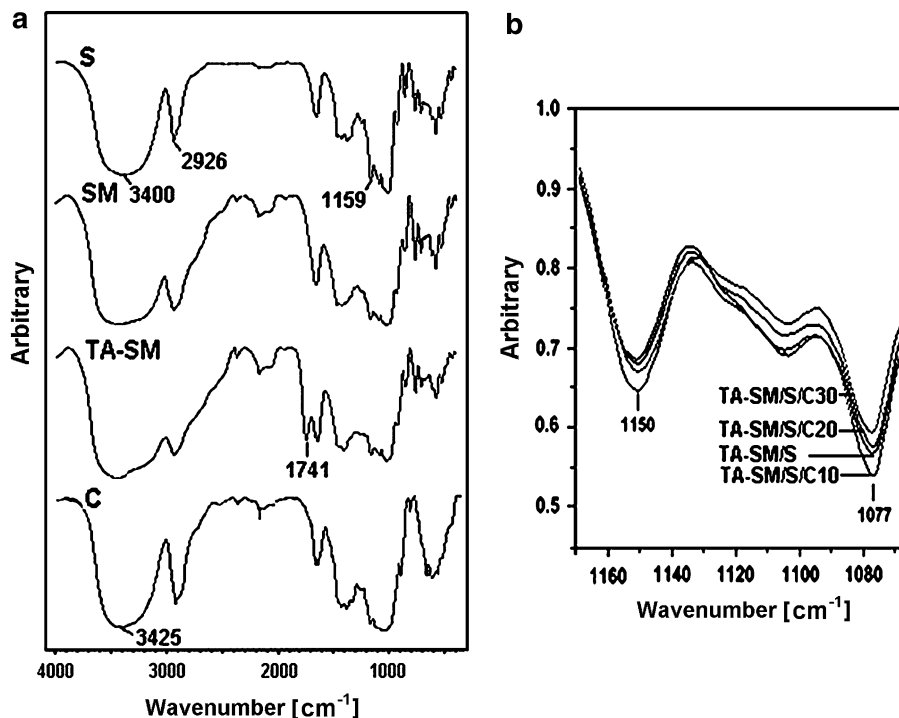
The neat starch and starch composite films present similar features in the two FTIR spectral regions, with the exception of the peaks related to the absorptions of the hydroxyl groups, at 1,650 and 1,017 cm^{-1}. The band at 1,017 cm^{-1}, associated with the C–OH bond, shows significant changes in the relative intensity of the doublet in agreement with the report of Van Soest et al. [26].

For TA-SM powders, a new peak occurred at 1,742 cm^{-1} is assigned to C=O stretching vibration, being an evidence of reaction between SM and TA. In S and SM, the oxygen of the C–O–C group could form the hydrogen-bond interaction with the hydroxyl groups, while the ester bonds in TA-SM as the cross-linking of starch sterically hindered this hydrogen-bond interaction. According to Huang et al. [27], the weakening of this interaction made C–O bond stretching of the C–O–C group shifted to 1,020 cm^{-1}.

The bands mainly assigned to cellulose are in the vibration range of intra- and intermolecular hydrogen bonded OH-groups between 3,500 and 3,200 cm^{-1} [28, 29], in the fingerprint region such as those at 1,336, 1,320, 1,164 and 1,114 cm^{-1}, and in the range of C–O valence vibrations from 1,060 to 1,015 cm^{-1} (see Fig. 1a). Technical celluloses, such as bleached wood pulp, contain additional carbonyl and carboxyl groups as a result of the isolation and purification processes that play a significantly role in the processing of cellulose [30, 31]. The C–O–C pyranose ring skeletal vibration gives a prominent band at 1,059 cm^{-1}. Significantly, the absence of the band at 1,520 cm^{-1} in the spectrum revealed that the birch cellulose is free of residual lignin.

Figure 2b shows the FTIR spectra of SM/S, TA-SM/S and TA-SM/S/cellulose films. First of all, we should mention that the starch composite films containing cellulose as filler (TA-SM/S/cellulose) exhibited almost the same FTIR spectra as the TA-SM/S film due to the chemical similarities between starch and cellulose. Through addition of glycerol, new hydrogen bonds are formed. The bands at 1,652 and 1,457 cm^{-1} were assigned to the O–H bending of water and CH$_2$, respectively. All peaks shifted to a lower wave-number than those of starch. This indicated that new hydrogen bonds were formed between components in the composite films. The band located at 1,081 cm^{-1} (in S, SM, TA-SM) for C–O stretching is shifted to 1,077 cm^{-1} in the TA-SM/S and TA-SM/S/cellulose composite films. The absorption band located at 995 cm^{-1} in SM/S and 999 cm^{-1} in TA-SM/S (assigned to C–O bond stretching vibrations of C–O–C group in the anhydroglucose ring of the starch) is shifted to 998 cm^{-1} in TA-SM/S/cellulose composite films as cellulose content changed from 0 to 30 wt %, this suggesting new interactions between cellulose and starch molecules.

The strong peaks observed at 998, 1,077 and 1,151 cm^{-1} are specific to the anhydroglucose ring in starch, although these signals could also be associated with the presence of glycerol molecules. Peak observed at around 1,059 cm^{-1} shifted to a higher wave-number value (around 1,151 cm^{-1}) in spectra for TA-SM/S/cellulose composites. This shift might be related to the weakening of hydrogen-bond interactions among cellulose molecules [29]. Absorption band observed at 896 cm^{-1} in the spectrum for birch cellulose, specific to glucose ring stretching, and C1–OH deformation

[32] is shifted to 861 cm^{-1} in TA-SM/S/cellulose composites.

All the changes in wave number indicate obvious interactions among the hydroxyl and carbonyl groups of the starch and cellulose components.

Film Surface Properties

Opacity is a very important characteristic for the films with applications in food packaging or food coating [33, 34]. This provides information on the size of dispersed particles within starch matrix. Thus, the particle sizes larger than the visible wavelength would obstruct light, leading to opaque composite materials.

Figure 3 illustrates the influence of cellulose fibers on the transparency of starch-based films. The transparency of the film can be decreased with an increase in the cellulose fiber content of the film. When light interacts with the film surface, it is reflected, absorbed, or transmitted and as a result a color, gloss, and transparency are exhibited by the film. The light diffusion occurs at the interface of the different film components and greatly impairs the light transmission. Cellulose fibers are not water soluble and randomly disperse within the starch matrix, and as such, exist in film as a discontinuous phase after drying. Therefore, cellulose fibers provide more interfacial area within the film structure. The light diffusion is increased and results in a reduction in film transparency. Overall, starch-based films maintain relatively transparency.

Contact Angle Measurements

Contact angle of water drop is an indication of the hydrophobic properties or wettability of the film surface.
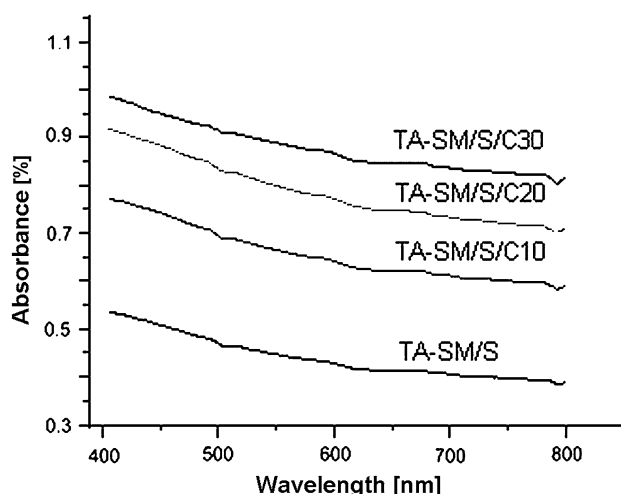
Table 1 Contact angle values of water droplet obtained for the starch-cellulose composite films

Sample	TA-SM/S	TA-SM/S/C10	TA-SM/S/C20	TA-SM/S/C30
Ethylene glycol	30.49	21.6	21.41	33.91
Water	23.28	38.15	45.9	86.48

The contact angles of water for the pulp samples increase as the purity of alpha cellulose decreases [35]. Alpha cellulose has the lowest measured contact angle of the wood components (26°). In the kraft delignifying process besides lignin, also hemicelluloses are partly removed, which makes the bleached kraft pulp a very pure form of alpha cellulose than holocellulose for example, which consists of alpha cellulose and hemicellulose, with just the lignin removed [35].

The use of starch modified with tartaric acid causes the increase of the contact angle between the water droplet and the surface over which it spread. This is because surface of film containing non-modified starch (SM/S) was more OH-rich macromolecules and has the capability to establish hydrogen bonds with water molecules. The presence of cellulose fibers slightly increased the contact angle between water and starch-cellulose composite materials surface as compared to TA-SM/S film (see Table 1). Cellulose in itself is hydrophilic and absorbs water fast. Kraft pulp, which consists mainly of cellulose, accordingly has a high affinity to water. At high cellulose content level, poor wetting properties of the starch-cellulose films are observed. This behavior could be due to the presence of some traces of hemicelluloses (xylan) in the cellulose used in composite materials.

Water Uptake

In a multiple biopolymer system, each biopolymer not only contributes to the film properties alone but also engages in biopolymer–biopolymer interactions that affect the overall system properties. Occasionally, these interactions are more important than individual actions.

Even though cellulose fibers were not expected to impart very high water resistance to the starch-based film, these were able to obviously improve water resistance of starch-based films. Because starch films are very sensitive to changes in moisture that results in changes in their mechanical properties, controlling the film moisture content is highly important. Hence, the water resistance provided by cellulose fibers is significant for new applications that are moisture sensitive such as gas selective membranes, ion channels, etc. Owing to the strong hydrophilic properties of starch molecules, a neat starch film displays high water absorbency. This factor impedes the application
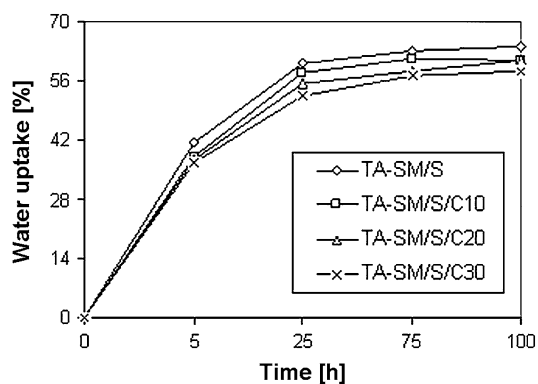

Fig. 3 Opacity values recorded for the starch-cellulose composite films

Fig. 4 Water uptake values recorded for the starch-cellulose composite films

of pure starch films for most non-absorbency applications. However, incorporation of various amounts of cellulose fibers into the starch matrix was able to reduce to a less extent the water absorbency of these films as shown in Fig. 4. Although cellulose is typically a hydrophilic polymer, the high crystallinity of the cellulose polymer and tight microfibrils structure within the fibers tend to discourage water absorbency when compared with that of amorphous starch. Nevertheless, there are still some hemicelluloses (xylan) in cellulose and these are more hydrophobe than cellulose, fact which could explain the results of water sorption experiments.

The water uptake-time curves exhibit two well-separated zones. At short times, below 25 h, the kinetics of absorption is very fast, whereas at long times, after 25 h, the kinetics of absorption is slow and leads to a plateau, corresponding to the equilibrium of water uptake. Therefore, the swelling of the films is reduced by incorporating cellulose into the plasticized starch matrix. The slightly improvement of surface and bulk-hydrophobation of the starch-based films, resulted from addition of cellulose, cannot be negligible.

The presence of cellulose causes a slightly increased water resistance and could improve the application property of the composite films. This behavior could be ascribed to the presence of strong hydrogen bonding interactions between starch and cellulose crystallites since the hydrogen bonding interactions in the composites tends to stabilize the starch matrix when it is subjected to highly moisturized atmosphere [24, 36, 37].

Mechanical Properties

The desired property of a food packaging material depends on the application. In general, a food packaging may be a non-deformable material to provide structural integrity or reinforce food structure, or a deformable film for other applications [38]. Poor strength properties (elastic modulus, tensile, compression) of neat starch films are major drawbacks for their use in diverse commercial applications. Improvements in the mechanical properties of film are therefore mandatory. In composite materials, the fine structure and interfacial properties of the components are extremely important for the attained mechanical properties. The ultimate strength of a composite is very sensitive to the dispersion of the reinforcing filler in the continuous phase. Similarly, poor dispersion of the components within composite film results in a weak film.

Each biopolymer not only contributes to the properties of composite films alone but also engages in biopolymer–biopolymer interactions which affect the mechanical properties of overall systems. In this multiple biopolymer system, cellulose and starch have good affinity to each other and obtain mutual property supplement, which can achieve the excellent tensile strength without affecting the extensibility of the films. The mechanical properties of the starch-cellulose composite films were measured in terms of tensile strength, elongation at break, Young's modulus according to ASTM D882-00 (ASTM D882-00 Standard Test Method for Tensile Properties of Thin Plastic Sheeting).

It is well accepted that tensile strength and Young's modulus of composites are influenced by the nature of matrix and the adhesion between fibers and matrix. The composite obtained from starch and tartaric acid modified starch shows a Young modulus of 160.4 MPa and a tensile strength of 5.9 MPa. It is known that well distributed particles with an adequate interfacial bonding between filler and matrix allows the effective transfer of stress through a shear mechanism from the matrix to the particles that can efficiently carry the load and enhance the strength of the composite [39].

As seen in Table 2, cellulose exhibited a significant reinforcement effect. With the increasing cellulose content, the tensile strength increased, while the elongation at break of the composites decreased. Cellulose has a more ribbon-like three-dimensional structure than starch and offers the possibility of more extensive hydrogen bonds. Thus, cellulose fibers addition induces variation of properties, due to

Table 2 Mechanical properties recorded for the starch-cellulose composite films

Sample	Young modulus (MPa)	Tensile strength (MPa)	Elongation at break (%)
TA-SM/S	160.4	5.9	52.5 ± 0.06
TA-SM/S/C10	747.4	9.9	11.2 ± 0.02
TA-SM/S/C20	965.8	14.8	4.5 ± 0.03
TA-SM/S/C30	1109.9	15.1	2.4 ± 0.02

the formation of a three-dimensional network between the different carbohydrates through hydrogen bonds. When the cellulose content varied from 10 to 20 wt %, the tensile strength increased significantly from 9.9 to 14.8 MPa. This evolution may be ascribed to the good interfacial interaction between cellulose and the starch polymers due to their similar structures [36]. Cellulose takes effects of the physical joints which improve the tensile strength, but decreases the flexibility of starch molecules, with effects on the elongation at break. Reinforcement of the starch-based films with 30 % cellulose caused a sevenfold increase in the elastic modulus and a significant improvement of tensile strength (2.5 times).

Thermal Properties

Thermal behavior of the starch-cellulose composite films was investigated to evaluate their thermal stability and degradation profiles. DSC thermograms from the first and second heating scans of the composites are shown in Fig. 5a, b. Thermograms indicated partial miscibility of cellulose and starch in the amorphous phase at the molecular level for all composite films and both polymers preserved a homogeneous material throughout the heating cycle, because phase separation (separated melting peaks) between the two biopolymers in composite films was not observed. Starch could undergo two endothermic events which are melting of amylopectin between 50 and 120 °C and that of amylose between 120 and 170 °C [40]. The increase in glass transition temperature (Tg) with increasing cellulose amount in composite samples can be attributed to anti-plasticization of amylopectin-rich domains by incorporating the cellulose fibers.
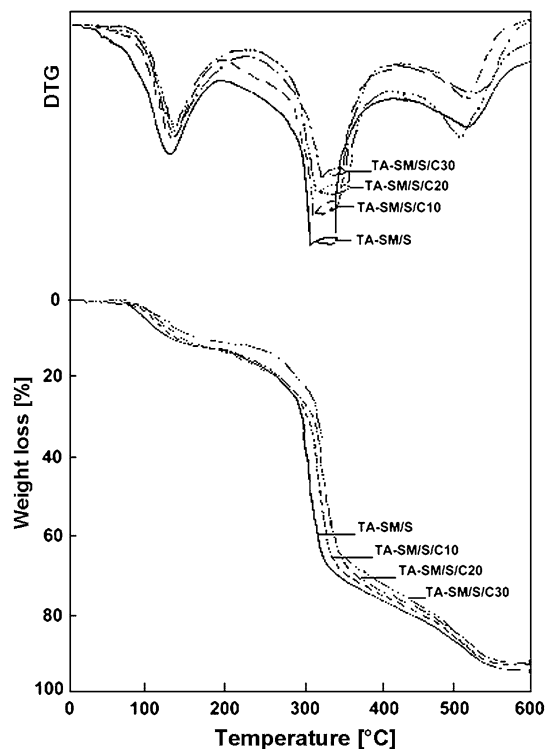

Fig. 6 TG curves recorded for the TA-SM/S, TA-SM/S/C10, TA-SM/S/C20 and TA-SM/S/C30 composite films

The effect of incorporation of cellulose into starch matrix can be seen as a shift in the endothermic transition range, due to the strong affinity of amylopectin molecules towards cellulose fibers through high density of hydroxyl groups which could reduce the global mobility of amylopectin domains. It seems that in the starch-cellulose
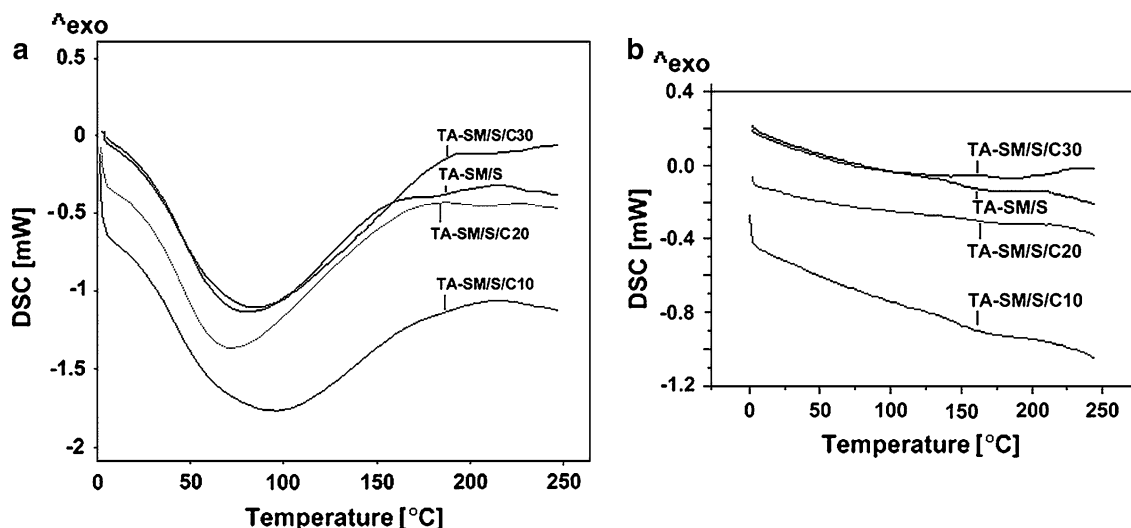

Fig. 5 DSC thermograms, first (a) and second heating (b) scans, for starch-cellulose composite films

composites the migration of glycerol molecules towards surface of cellulose fibers is higher than starch matrix. In such a system, at the interface, crystalline (ordered) coating of glycerol and amylopectin could result in restricted mobility on the surface of cellulose fibers. This was confirmed in the tensile properties as decrease in elongation (%).

A wide temperature range of endothermic thermal transition can be observed for all composite samples (Fig. 5a—first heating scan). This behavior can be attributed to the migration of solvents (water, glycerol) from samples, the wider temperature range (70–120 °C) being noticed for TA-SM/S/C30 sample.

It could also be seen in the DSC curves of the starch-cellulose films (Fig. 5b—for second heating scan) that the temperature corresponding to Tg increased when the cellulose content is higher, probably due to the increasing molecular weight of polymer in amorphous region of the composite matrix, interactions between components and mechanical reinforcing effects of cellulose. TA-SM/S composite sample exhibited a lower Tg value (149.17 °C) by comparison with samples containing cellulose, their Tg values being 160.3 °C (TA-SM/S/C10), 170.33 °C (TA-SM/S/C20), and 175.2 °C (TA-SM/S/C30), respectively. It seems that the presence of the cellulose within the starch matrix influenced the size and amount of crystalline regions formed in the starch matrix. The increase in Tg dependence of the cellulose addition might be attributed to the interactions between starch and cellulose, resulting in a decrease in the mobility of starch macromolecules.

Samples for thermogravimetric analysis were the same as those of FTIR spectroscopy investigation. A small weight loss of about 2–5 % below 100 °C is assigned to the release of moisture from the samples. All of the composite samples show one-stage degradation within the range of 230–420 °C (Fig. 6). The residual weights of the composite films beyond 500 °C increase slightly with increasing cellulose content in the composite films. The maximum decomposition temperatures of the composite films (Tmax = 320–330 °C) are higher than that of modified starch/plasticized starch (Tmax = 310 °C), showing relatively high thermal stability because of the enhancement of inter-molecular hydrogen bonds among biopolymers in the composite films.

Thermograms recorded for the different starch-cellulose composite films show higher degradation temperatures (main temperature domain) with increasing cellulose content level. Looking at the residual mass after heating composite samples up to 600 °C, a lower residual weight is observed for the TA-SM/S composite film which has no cellulose in composition. This behavior reveals that some hydroxyl groups in the cellulose polymer chains have interacted with the other components within the starch matrix.

Conclusions

The incorporation of cellulose within starch matrix modified the physical and chemical properties of starch-based composite materials bringing significant improvements while maintaining the natural advantages of starch films. In this paper, starch-cellulose composite materials were prepared from modified starch microparticles originating from starch previously cross-linked by reaction with tartaric acid as filler within a glycerol plasticized-corn starch matrix by the casting process. Cellulose, originating from a bleached birch industrial pulp, with different content levels, was incorporated within the polymer matrix mentioned above.

X-ray diffraction and FTIR spectroscopy evidenced the changes in the structure of starch, starch microparticles and modified starch microparticles. The absorption peaks corresponding to the hydroxyl, carbonyl and ether groups in starch have a tendency to shift to higher wave number for the starch-cellulose composite materials, indicating the existence of a hydrogen–bonding interaction between starch and cellulose.

Mechanical tests, wettability, and water sorption tests, as well as thermal properties of starch-cellulose composite materials were investigated. Even though cellulose fibers were not expected to impart very high water resistance to the starch-based film, these were able to obviously improve water resistance of starch-based films. Another significant effect of cellulose fiber is the stabilization of film water resistance although there is a slight decrease in film transparency. Cellulose fiber tends to increase hydrophobic properties of the starch-based film, but this effect is limited. Film transparency is decreased with an increase in cellulose content in films, and this negative effect could be further enhanced by high cellulose content.

Due to the strong intermolecular hydrogen bonds, the thermal stability of the starch-cellulose composite films is improved comparatively with those without cellulose. A significant increase of the Young modulus and the maximum tensile strength as well as a significant diminution of the percentage of elongation at break with increasing the cellulose content was observed for starch-based composite films. Thus, the addition of cellulose fibers to starch-based films represents a promising way to obtain resistant and more stable films. Nevertheless, the understanding of the basic mechanical properties of cellulose and starch has a real significance for the development of biodegradable materials to replace synthetic polymers for packaging applications.

References

1. Yang KK, Wang XL, Wang YZ (2007) J Ind Eng Chem 13:485
2. Pandey JK, Kumar AP, Misra M, Mohanty AK, Drzal LT, Singh RP (2005) J Nanosci Nanotechnol 5:497
3. John MJ, Thomas S (2008) Carbohydr Polym 71:343
4. Romero-Bastida CA, Bello-Pérez LA, García MA, Martino MN, Solorza-Feria J, Zaritaky NE (2005) Carbohydr Polym 60:235
5. Rioux B, Ispas-Szabo P, Ait-Kadi A, Mateescu M, Juhasz J (2002) Carbohydr Polym 50:371
6. Wang LF, Pan SY, Hu H, Miao WH, Xu XY (2010) Carbohydr Polym 80:174
7. Yu J, Wang N, Ma X (2005) Starch 57:494
8. Chen CH, Lai LS (2008) Food Hydrocoll 22:1584
9. Rhim JW (2007) Food Sci Biotechnol 16:691
10. Liu D, Zhang L (2006) Macromol Mat Eng 291:820
11. Bertuzzi MA, Armada M, Gottifredi JC (2007) J Food Eng 82:17
12. Liu D, Wu Q, Chen H, Chang PR (2009) J Colloid Interface Sci 339:117
13. Orts WJ, Shey J, Imam SH, Glenn GM, Guttman ME, Revol JF (2005) J Polym Environ 13:301
14. Teixeira EM, Pasquini D, Curvelo AAS, Corradini E, Belgacem MN, Dufresne A (2009) Carbohydr Polym 78:422
15. Bledzki AK, Gassan J (1999) Progr Polym Sci 24:221
16. Samir M, Alloin F, Dufresne A (2005) Biomacromolecules 6:612
17. John MJ, Anandjiwala RD, Pothan LA, Thomas S (2007) Compos Interface 14:733
18. Chakraborty A, Sain M, Kortschot M, Cutler S (2007) J Biobased Mat Bioenergy 1:71
19. Ma X, Chang PR, Yu J, Stumborg M (2009) Carbohydr Polym 75:1
20. Dufresne A, Vignon MR (1998) Macromolecules 31:2693
21. Ma XF, Jian RJ, Chang PR, Yu JG (2008) Biomacromolecules 9:3314
22. Spiridon I, Teacă C-A, Bodîrlău R (2011) J Mat Sci 46:3241
23. Vermeylen R, Derycke V, Delcour JA, Goderis B, Reynaers H, Koch MHJ (2006) Biomacromolecules 7:1231
24. Van Soest JJG, Vliegenthart JFG (1997) Trends Biotechnol 15:208
25. Fang JM, Fowler PA, Tomkinson J, Hill CAS (2002) Carbohydr Polym 47:245
26. Van Soest JJG, Tournois H, de Wit D, Vliegenthart JFG (1995) Carbohydr Res 279:201
27. Huang MF, Yu JG, Ma XF (2004) Polymer 45:7017
28. Hinterstoisser B, Salmén L (1999) Cellulose 6:251
29. Kondo T, Sawatari C (1996) Polymer 37:393
30. Klemm D, Heublein B, Fink HP, Bohn A (2005) Angew Chem Int Ed 44:3358
31. Rőhrling J, Potthast A, Rosenau T, Sixta H, Kosma P (2002) Lenzinger Berichte 81:89
32. Pandey KK (1999) J Appl Polym Sci 71:1969
33. Mali S, Grossmann MVE, Garcia MA, Martino MN, Zaritzky NE (2004) Carbohydr Polym 56:129
34. Gontard N, Guilbert S, Cuq JL (1992) J Food Sci 57:190
35. Liukkonen A (1997) Scanning 19:411
36. Ma X, Yu J, Kennedy JF (2005) Carbohydr Polym 62:19
37. Lu YS, Weng LH, Cao XD (2005) Macromol Biosci 5:1101
38. Atwell WA, Hood LF, Lineback DR, Varrianomarston E, Zobel HF (1988) Cereal Foods World 33:306
39. Angles MN, Dufresne A (2001) Macromolecules 34:2921
40. Silverio J, Svensson E, Eliasson AC, Olofsson G (1996) J Therm Anal Calorim 47:1179